200912039A

厚生労働科学研究費補助金

医療機器開発推進研究事業

「ＲＮＡ創薬を支援するバイオイメージング技術の確立」に関する研究

平成２１年度　総括研究報告書

研究代表者　浅井　知浩

平成２２（２０１０）年　４月

目　　次

厚生労働科学研究費補助金（医療機器開発推進研究事業）
統括研究報告書

ＲＮＡ創薬を支援するバイオイメージング技術の確立（H20-ナノ-若手-007）

主任研究者　　浅井 知浩　静岡県立大学大学院薬学研究科講師

研究要旨　本研究ではsiRNAの体内動態を非侵襲的、リアルタイムかつ高感度に解析する技術の確立を目的とし、siRNA の ^{18}F ポジトロン標識体の開発ならびにポジトロン断層法（positron emission tomography; PET）による動態解析技術の構築を目指した。事業計画の初年度は、siRNA ポジトロン標識体の開発に成功し、PET 解析に向けた予試験を実施した。2 年目となる本年度は、siRNA 体内動態の PET 解析法の構築、PET と蛍光法の比較、および各種ベクターに搭載した siRNA の PET 体内動態解析を重点的に実施した。siRNA の体内動態を解析するにあたっては、siRNA ベクターとしてカチオニックリポソームとポリエチレングリコール（PEG）修飾リポソームを用いた。これら物性のまったく異なるリポソームを siRNA ベクターとして用いることで siRNA の体内動態を比較評価した。予め siRNA の血清中での安定性について *in vitro* で検討し、siRNA 単体では血清中で速やかに分解されるが、ベクターに搭載した siRNA は安定であることを明らかにした。次に ^{18}F ポジトロン標識 siRNA をマウスに尾静脈内投与し、その体内動態を簡易型二次元 PET 装置（planar positron imaging system: PPIS）を用いて解析した。その結果、siRNA 単体では投与後速やかに腎臓に集積し、膀胱に移行する様子が観察された。カチオニックリポソームに搭載した siRNA は投与後速やかに肺に集積し、そのまま肺に留まる様子が観察された。PEG 修飾リポソームに搭載した siRNA では、全身から強いシグナルが検出され、PEG 修飾リポソームの特徴である長期血中滞留性を示すイメージデータが得られた。PET 計測終了後に動物を解剖して各組織の放射線量を測定した結果、イメージデータとの整合性が得られた。以上のように、用いたベクターの性質に依存して siRNA の体内動態が変化する様子を非侵襲的かつリアルタイムに明らかすることに成功した。一方、PET 解析データとの比較検証を目的とし、近赤外蛍光 *in vivo* イメージング法を利用して siRNA の体内動態を解析した。近赤外蛍光色素 Alexa750 をアンチセンス鎖 3'末端に結合した siRNA をイメージングに用いた。標識および測定装置以外は PET 解析と全く同様の条件で動態を解析した。その結果、PET と蛍光法のデータ間には測定原理に基づく差が生じるものの、蛍光法は PET 解析データの検証に有効であることを明らかになった。以上の研究成果は、2 年目までの研究事業計画がほぼ予定通りに遂行されていることを示しており、siRNA 体内動態の PET 解析技術の確立に向けて、着実に研究成果が得られた。

A. 研究目的

RNA 干渉は、次世代の医療技術として有望視されており、いわゆる RNA 創薬に関する研究は医療応用に向けて着実に進展している。small interfering RNA（siRNA）の医療応用を促進するには、疾患部位に必要量の siRNA を送達することを目的とした核酸デリバリーシステムの開発が重要課題といえる。これまで siRNA の運搬体（リポ

ソーム、高分子ミセル等のベクター）の体内動態は詳細に解析されてきたが、主薬である siRNA 本体の体内動態は未知のことが多い。そこで本研究では siRNA の体内動態を非侵襲的、リアルタイムかつ高感度に解析する技術の確立を目的とし、siRNA の ^{18}F ポジトロン標識体の開発ならびにポジトロン断層法（positron emission tomography; PET）による動態解析技術の構築を目指した。本研究の特徴は、1）他の類似技術よりも比較的高感度なイメージング技術であること、2）ベクターではなく主薬である siRNA の動態解析技術であること、3）疾患、標的配列、ベクターによって限定されず応用範囲が広いこと、4）ヒトマイクロドーズ試験への発展性などが挙げられる。

本研究の目標達成によって siRNA の体内動態データが取得可能となれば、治療効果を予測するうえでも DDS 医薬品の製剤設計にフィードバックするうえでも貴重な情報が得られることになり、動物を利用したヒトでの有効性・問題点評価に有効であると考えられる。さらに PET は、がん検診でヒトでの使用実績があるうえ、今後はマイクロドーズ試験への応用が期待されており、siRNA の PET による動態解析は先見性の高い試みといえる。短半減期のポジトロンを使用する PET 解析は、長時間の動態解析には向かないが、被ばくの観点からはヒトへの応用に向いた動態解析技術といえる。3 ヶ年計画の研究事業の具体的な検討項目としては、siRNA ポジトロン標識体の開発、siRNA 体内動態の PET 解析技術の確立、蛍光 *in vivo* イメージングとの比較、各種ベクターに搭載した標識 siRNA の動態解析、病態モデル動物における siRNA の動態解析を計画している。

研究計画の 2 年目となる本年度は、siRNA 体内動態の PET 解析法の構築、PET と蛍光法の比較、および各種ベクターに搭載した siRNA の PET 体内動態解析を重点的に実施した。

B. 研究方法

（1）siRNA ポジトロン標識体の調製

アンチセンス鎖 3'末端をアミノ化した siRNA を北海道システム・サイエンス社に委託して合成した。siRNA の配列は、スクランブル（コントロール）配列を用いた。このアミノ化 siRNA と[^{18}F]-コハク酸イミド誘導体をホウ素緩衝液中で混合し、室温にて 20 分間静置して反応させた。次に限外濾過操作によって未反応の ^{18}F を除去し、ポジトロン標識 siRNA（^{18}F-siRNA）を得た。なお、^{18}F を取り扱う実験は、浜松ホトニクス株式会社中央研究所 PET センターの研究協力を得て実施した。

（2）リポソーム化 siRNA の調製

カチオン性脂質 DOTAP とコレステロールを *t*-ブタノール溶液中で混合し、一晩凍結乾燥した。RNase フリーのリン酸緩衝液で水和後、リポソームの粒子径をエクストルージョン法にて約 100 nm に調整した。^{18}F-siRNA とリポソームを室温にて 20 分間インキュベートし、リポソーム化 siRNA を調製した（カチオニックリポソーム）。また、リポソーム化 siRNA 溶液に MPEG6000-DSPE を加え、60°C で 10 分間インキュベートして PEG 修飾を施した（PEG 修飾リポソーム）。各リポソーム化 siRNA の粒子径および ζ 電位は、Zetasizer Nano ZS を用いて計測した。

（3）リポソーム化 siRNA の安定性

siRNA 溶液あるいはリポソーム化 siRNA 溶液に最終濃度 90%血清となるように血清を混和し、37 °C にて 1 時間インキュベートした。siRNA を抽出した後、ポリアクリルアミド電気泳動によって分離し、Ethidium Bromide により染色した。各バンドの蛍光強度は、LAS-3000 を用いて測定した。

（4）siRNA 体内動態の PET 解析

^{18}F-siRNA 単体ならびに上述のリポソームに搭載した ^{18}F-siRNA の体内動態を解析した。5 週齢雄性 BALB/c マウスに各サンプルを尾静脈内に設置したカニューレより投与し、簡易型 2 次元 PET 装置（planer positron imaging system）を用いて体

内動態を解析した。1時間のPET計測終了後にマウスを解剖し、各臓器における放射活性をガンマカウンターにて測定した。

(5) 蛍光標識siRNAの*in vivo*イメージング

近赤外蛍光色素であるAlexa750で標識したsiRNAを用いて、siRNA搭載リポソームを調製した。蛍光*in vivo*イメージングの装置としては、Xenogen社のIVIS® Luminaを用いた。5週齢雄性BALB/cマウスに尾静脈内投与し、投与直後より経時的にsiRNAの体内動態を観察した。1時間のイメージング終了後にマウスを解剖し、各臓器における蛍光強度を*ex vivo*にて評価した。

・倫理面への配慮

当該研究に関して、すべての動物実験プロトコールは、所属機関における動物実験委員会による審査・承認を受けている。また、動物愛護の精神にのっとり、実験により派生する恐怖・苦痛をできるかぎり軽減できる方法を選択して用いた。

C. 研究結果

(1) siRNA体内動態のPET解析

はじめにsiRNAの血清中での安定性について*in vitro*で検討した結果、siRNA単体では血清中で速やかに分解されるが、リポソームベクターに搭載したsiRNAは血清中で安定に存在しうることが明らかとなった。次に、^{18}F-siRNA単体ならびにリポソームに搭載した^{18}F-siRNAのマウスにおける体内動態をPET解析し、その結果を図1に示した。siRNA単体では投与後速やかに腎臓に集積し、膀胱に移行する様子が観察された。カチオニックリポソームに搭載したsiRNAは投与後速やかに肺に集積し、そのまま肺に留まる様子が観察された。さらに、PEG修飾リポソームに搭載したsiRNAでは、PET計測終了時の1時間後においても全身からシグナルが検出され、PEG修飾リポソームの特徴である長期血中滞留性を反映したイメージデータが得られた。また、カチオニックリポソームとの比較では、初回通過臓器である肺に捕捉されない分、肝臓や脾臓等への分布が検出された。PET解析後に各臓器における放射活性を測定した結果、^{18}Fの臓器分布はイメージデータと一致しており、両データ間の整合性が確認された。

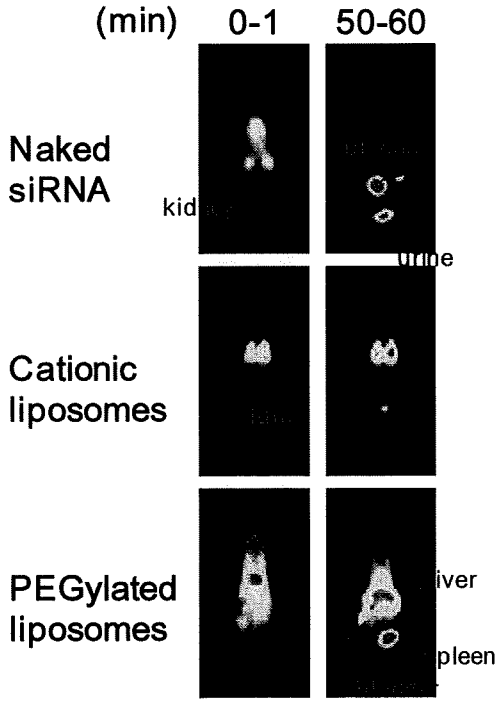

図1 ^{18}F標識siRNAを用いたPETイメージデータ

(2) 近赤外蛍光イメージング法との比較

Alexa750標識siRNAをマウスに尾静脈内投与し、IVIS® Luminaを用いてその体内動態を解析した。標識および測定装置を除き、PET解析とまったく同様の条件で実験を行った。その結果、PET解析法とは異なり、蛍光法では体表面に近い臓器からのシグナルが強調された(図2)。蛍光法では体表面からの深度の影響が大きいため、非侵襲的なリアルタイムイメージングと解剖後の*ex vivo*データに差が生じた。*in vivo*イメージングでは、体表面に近い膀胱のシグナルが過度に強調され、その他の臓器分布のシグナルは相対的に減弱し

ていた。PETイメージングで確認されたPEG修飾リポソームの長期血中滞留性は、近赤外蛍光の *in vivo* イメージングでは捉えることができなかった。しかしながら、蛍光法においても解剖後の *ex vivo* データは、PETイメージデータおよびPET解析後の臓器分布データとほぼ一致していた。

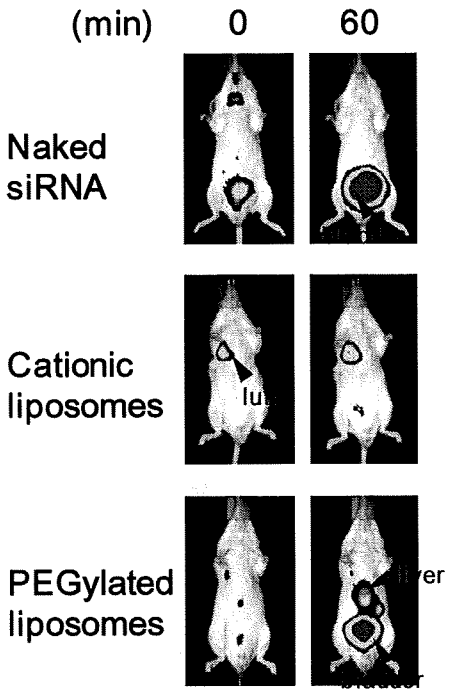

図2　Alexa750標識siRNAを用いた近赤外蛍光イメージデータ

D. 考察

事業計画の初年度に開発した ^{18}F-siRNAを用い、各種ベクターに搭載したsiRNA体内動態のPET解析、PETと蛍光法の比較について重点的に実施した。siRNAの体内動態を解析するにあたり、カチオニックリポソームとポリエチレングリコール修飾リポソームをsiRNAのベクターとして用い、siRNA単体の体内動態と比較検討した。これまでの検討結果より、カチオニックリポソームを小動物に静脈内投与した場合、その表面電荷の影響によって初回通過臓器である肺へ集積することが明らかとなっている。一方、PEG修飾によってその電荷をマスクしたリポソームは、肺や他の細網内皮系組織による捕捉を回避して高い血中滞留性を示し、カチオニックリポソームとは顕著に異なる体内動態を示すことが明らかとなっている。今回、このような体内動態がまったく異なるリポソームをsiRNAベクターとして用い、^{18}F-siRNAの体内動態を比較評価した。結果に示したように、^{18}F-siRNAは用いたベクターの性質に依存した体内動態を示し、siRNAが血清中で分解を受けず、ベクターとともに存在していることが示唆された。今回得られたPETイメージデータは、解剖後の各臓器における放射活性データや蛍光法の *ex vivo* データとも結果が一致しており、^{18}F-siRNAの体内分布を反映しているものと考えられる。以上より、用いたベクターの性質に依存してsiRNAの体内動態が変化する様子を非侵襲的かつリアルタイムにPETイメージングすることに成功したと考えられる。

一方で、PETと蛍光法の比較についても検討を実施し、PET解析技術の有効性を評価した。非侵襲的な *in vivo* イメージデータ間で両者を比較した場合は、体表面からの深度の影響を受けないPETが有利であることが明確に示された。PET解析データと蛍光法の *ex vivo* データが一致しているため、*in vivo* データ間の差は、siRNAの分布が実際に変化したわけではなく、測定原理に基づく差に由来したと考えられる。以上より、PETと蛍光法のデータ間には測定原理に基づく差が生じるものの、蛍光法はPET解析データの検証に有効であることが明らかとなった。なお、蛍光法は長時間の測定が可能など、PETとはまた異なる利点があり、それぞれの技術を組み合わせることで、より詳細な体内動態解析が可能になると考えられる。

本課題研究における検討を継続し、siRNA体内動態のPET解析技術の確立に至れば、治療効果を予測するうえでもDDS製剤の設計に情報をフィ

ードバックするうえでも極めて貴重な解析データが得られるようになる。したがって、siRNA やそのキャリアなどにおいて有望なシーズを保有している企業ならびに公的機関に対して魅力的な動態解析技術を提供できるようになる。医薬品候補の siRNA の体内動態に関して有益な情報が得られることにより、RNA 創薬の開発効率を高め、創薬の加速化に結び付くと考えられる。さらに PET 技術は、ヒトマイクロドーズ試験への応用に発展する可能性を有しており、これが実現すればさらなる開発効率の向上が期待できる。以上のように、本研究の目標が達成されることにより、国民を悩ます疾病の克服を目指した医薬品開発に大きな波及効果を生むことができる可能性がある。

E. 結論

事業計画の 2 年目の平成 21 年度までに、siRNA ポジトロン標識体の開発、siRNA 体内動態の PET 解析、リポソームベクターに搭載した siRNA の PET 動態解析、近赤外蛍光 *in vivo* イメージングを用いた PET 解析データの比較検証等をほぼ計画通りに実施してきた。3 年目の最終年度は、疾患モデル動物における siRNA 体内動態の PET 解析、新規ベクターに搭載した siRNA の動態解析等の応用研究に重点的に取り組み、本技術の有用性をより明確なものにする。本研究事業の目標を計画通りに達成し、開発する技術が RNA 創薬の加速化に繋がることを期待している。

F. 健康危険情報

なし

G. 研究発表

1. 論文発表

1) Hatanaka, K., Asai, T., Koide, H., Kenjo, E., Tsuzuku, T., Harada, N., Tsukada, H., Oku, N.: Development of double-stranded siRNA labeling method using positron emitter and its in vivo trafficking analyzed by positron emission tomography. *Bioconjug. Chem.* **21**, 756-763 (2010)

2) Koide, H., Asai, T., Hatanaka, K., Akai, S., Ishii, T., Kenjo, E., Ishida, T., Kiwada, H., Tsukada, H., Oku, N.: T cell-independent B cell response is responsible for ABC phenomenon induced by repeated injection of PEGylated liposomes. *Int. J. Pharm.* 392, 218-223 (2010)

3) Ishii, T., Asai, T., Urakami, T., Oku, N.: Accumulation of macromolecules in brain parenchyma in acute phase of cerebral infarction/reperfusion. *Brain Res.* **1321**, 164-168 (2010)

4) Shimizu, K., Osada, M., Takemoto, K., Yamamoto, Y., Asai, T., Oku, N.: Temperature-dependent transfer of amphotericin B from liposomal membrane of AmBisome to fungal cell membrane. *J. Control. Release*, **141**, 208-215 (2010)

5) Murase, Y., Asai, T., Katanasaka, Y., Sugiyama, T., Shimizu, K., Maeda, N., Oku, N.: A novel DDS strategy, "dual-targeting", and its application for antineovascular therapy. *Cancer Lett.*, **287**, 165-171 (2010)

2. 学会発表

・招待講演

1) がんの RNA 干渉治療を目的とした全身投与型 siRNA ベクターの開発. 日本薬学会第 130 年会, 一般シンポジウム S10「異分野技術の融合による次世代の医療基盤技術の構築に向けて」, 2010 年 3 月 29 日, 岡山

2) Development of PET technology to determine pharmacokinetics of siRNA medicine. APSTJ Global Education Seminar East 2009-03, 5

October, 2009, Tokyo, Japan

3) siRNA体内動態のPET解析と新規ベクターの開発. 第25回日本DDS学会, ワークショップ1「核酸医薬のDDS」, 2009年7月3日, 東京

・一般講演

1) Asai, T., Hatanaka, K., Koide, H., Shimizu, K., Harada, N., Tsukada, H., Oku, N.: PET technology to determine pharmacokinetics of liposomal siRNA. 4th International Liposome Society Conference, 2009年12月14日, London, UK

2) Kenjo, E., Asai, T., Matsushita, S., Dewa, T., Nango, M., Maeda, N., Oku, N.: Development of siRNA delivery system using novel polycation liposomes for cancer therapy. 4th International Liposome Society Conference, 2009年12月14日, London, UK

3) Koide, H., Asai, T., Yokoyama, M., Ishida, T., Kiwada, H., Oku, N.: Elucidation of ABC phenomenon caused by repeat injection of PEGylated nanocarrier. 4th International Liposome Society Conference, 2009年12月14日, London, UK

4) Tsuzuku, T., Asai, T., Matsushita, S., Dewa, T., Nango, M., Maeda, N., Oku, N.: Development of in vivo delivery system for siRNA-based cancer therapy. 第31回生体膜と薬物の相互作用シンポジウム, 2009年11月30日, 大阪

5) 畑中剣太朗, 浅井知浩, 小出裕之, 原田典弘, 塚田秀夫, 奥 直人: RNA創薬研究におけるPETイメージング技術の開発. 第9回放射性医薬品・画像診断薬研究会, 2009年11月14日, 京都

6) Kato, K., Uchida, M., Sumino, A., Dewa, T., Asai, T., Oku, N., Nango, M.: Polyamine-lipid/DNA Complexes as Gene Carriers: Morphological Observation of the Complexes by Using AFM. 3rd International Symposium on Nanomedicine, 2009年11月5日, 岡崎

7) Dewa, T., Kato, K., Uchida, M., Sumino, A., Asai, T., Oku, N., Nango, M.: Liposomal Polyamine-Dialkyl Phosphate Conjugates as Effective Gene Carriers: Chemical Structure, Morphology, and Gene Transfer Activity. 3rd International Symposium on Nanomedicine, 2009年11月5日, 岡崎

8) 出羽毅久, 加藤清志, 内田みさ, 角野 歩, 浅井知浩, 奥 直人, 南後 守: ポリアミン脂質による遺伝子送達とDNA複合体形態の直接観察, 第58回高分子討論会. 2009年9月16日, 熊本

9) 出羽毅久, 加藤清志, 内田みさ, 角野 歩, 浅井知浩, 奥 直人, 南後 守: ポリアミン脂質-DNA複合体のAFMによる形態観察と遺伝子送達能. 第19回バイオ・高分子シンポジウム, 2009年7月29日, 東京

10) Hatanaka, K. Asai, T., Koide, H., Harada, N., Tsukada, H., Oku, N.: Development of PET technology for the pharmacokinetic study of siRNA medicine. 36th Annual Meeting & Exposition of Controlled Release Society, 2009年7月20日, Copenhagen, Denmark

H. 知的財産権の出願・登録状況

なし

研究成果の刊行に関する一覧表

雑誌

発表者氏名	論文タイトル名	発表誌名	巻号	ページ	出版年
Hatanaka, K., Asai, T., Koide, H., Kenjo, E., Tsuzuku, T., Harada, N., Tsukada, H., Oku, N.	Development of double-stranded siRNA labeling method using positron emitter and its in vivo trafficking analyzed by positron emission tomography.	*Bioconjug. Chem.*	**21**	756-763	2010
Koide, H., Asai, T., Hatanaka, K., Akai, S., Ishii, T., Kenjo, E., Ishida, T., Kiwada, H., Tsukada, H., Oku, N.	T cell-independent B cell response is responsible for ABC phenomenon induced by repeated injection of PEGylated liposomes.	*Int. J. Pharm.*	**392**	218-223	2010
Ishii, T., Asai, T., Urakami, T., Oku, N.	Accumulation of macromolecules in brain parenchyma in acute phase of cerebral infarction/reperfusion.	*Brain Res.*	**1321**	164-168	2010
Murase, Y., Asai, T., Katanasaka, Y., Sugiyama, T., Shimizu, K., Maeda, N., Oku, N.	A novel DDS strategy, "dual-targeting", and its application for antineovascular therapy.	*Cancer Lett.*	**287**	165-171	2010
Shimizu, K., Osada, M., Takemoto, K., Yamamoto, Y., Asai, T., Oku, N.	Temperature-dependent transfer of amphotericin B from liposomal membrane of AmBisome to fungal cell membrane.	*J. Control. Release*	**141**	208-215	2010

Development of Double-Stranded siRNA Labeling Method Using Positron Emitter and Its In Vivo Trafficking Analyzed by Positron Emission Tomography

Kentaro Hatanaka,[†] Tomohiro Asai,[†] Hiroyuki Koide,[†] Eriya Kenjo,[†] Takuma Tsuzuku,[†] Norihiro Harada,[‡] Hideo Tsukada,[‡] and Naoto Oku*,[†]

Department of Medical Biochemistry and Global COE Program, Graduate School of Pharmaceutical Sciences, University of Shizuoka, 52-1 Yada, Suruga-ku, Shizuoka-city, Shizuoka 422-8526, Japan, and PET Center, Central Research Laboratory, Hamamatsu Photonics K.K., 5000 Hirakuchi, Hamakita-ku, Hamamatsu-city, Shizuoka 434-8601, Japan. Received December 7, 2009; Revised Manuscript Received February 8, 2010

Pharmacokinetic study of small interfering RNA (siRNA) is an important issue for the development of siRNAs for use as a medicine. For this purpose, a novel and favorable positron emitter-labeled siRNA was prepared by amino group-modification using *N*-succinimidyl 4-[fluorine-18] fluorobenzoate ([^{18}F]SFB), and real-time analysis of siRNA trafficking was performed by using positron emission tomography (PET). Naked [^{18}F]-labeled siRNA or cationic liposome/[^{18}F]-labeled siRNA complexes were administered to mice, and differential biodistribution of the label was imaged by PET. The former was cleared quite rapidly from the bloodstream and excreted from the kidneys; but in contrast, the latter tended to accumulate in the lungs. We also confirmed the biodistribution of fluorescence-labeled naked siRNA and cationic liposome/siRNA complexes by use of a near-infrared fluorescence imaging system. As a result, a similar biodistribution was observed, although quantitative data were obtained only by planar positron imaging system (PPIS) analysis but not by fluorescence in vivo imaging. Our results indicate that PET imaging of siRNA provides important information for the development of siRNA medicines.

INTRODUCTION

Small interfering RNA (siRNA) is a short double-stranded nucleic acid molecule that induces sequence-dependent gene silencing (*1, 2*), and gene therapy using siRNA is expected to be a novel treatment strategy for various diseases (*3*). However, the degradation of naked siRNA after administration into the bloodstream of human and animals readily occurs due to nucleases in the blood. Furthermore, siRNA poorly penetrates the plasma membranes of target cells, thus making difficult the delivery to the cytosol of targeted cells for effective gene knockdown. Therefore, a delivery system of siRNA molecules is considered to be indispensable for establishing siRNA therapy. Many studies on the in vivo application of siRNA using chemical modification (*4*) or drug delivery system (DDS) carriers such as liposomes (*5*) and micelles (*6*) for efficacious delivery and gene silencing have been reported. Cationic liposomes or micelles are representative carriers having electric charges on their surface. Because siRNA possesses polyanionic charges, it electrostatically interacts with cationic carriers used for RNA interference (RNAi). Pharmacokinetic studies on siRNA/carrier complexes have been performed by using fluorescence- or radioisotope-labeled carriers or carrier-entrapped imaging agents for magnetic resonance imaging. The techniques of carrier-labeling, however, do not always reflect the biodistribution of siRNA, since there is a chance that the siRNA may become detached from the carrier in the bloodstream, especially when the siRNA is bound to the surface of cationic carriers. To evaluate the in vivo behavior of siRNA itself, the trafficking of it is carried out by near-infrared fluorescence (NIRF) imaging (*7*). However, like fluorescence imaging, NIRF imaging is affected by tissue depth to some extent, and therefore, quantitative data are difficult to obtain. In addition, although the NIRF imaging method is applicable for use on nonhuman primates, the method for human use has not yet been established.

To obtain precise pharmacokinetic information on siRNA molecules or their carriers in vivo, positron emission tomography (PET) is one of the ideal techniques. PET enables the determination of the real-time biodistribution and topical accumulation of positron emitter-labeled compound noninvasively. This technique can be applied in preclinical studies, in which a drug candidate labeled with a positron emitter is injected into animals. The circulation profile, biodistribution in various tissues, and eventual elimination of the drug candidate from the body can be monitored noninvasively in the same animal. Furthermore, certain positron emitter-labeled new drug candidates can be used for microdosing studies in humans. Such phase zero studies enable the investigator to reduce the rate of dropout of drug candidates in further clinical studies. For the pharmacokinetic study of DDS carriers, we previously reported a novel [^{18}F]-probe for labeling the lipid assembly carriers for PET analysis (*8*). As mentioned above, since siRNA may possibly dissociate from its carrier and be degraded by plasma nucleases after injection into the bloodstream, we have sought to label siRNA with a positron emitter for the analysis of siRNA trafficking in vivo. The pharmacokinetic information on siRNA molecules, like that of the carrier, is considered to be critical and indispensable for the development of siRNA medicines.

Recently, Bartlett et al. labeled the sense strand of siRNA with copper-64 by using 1,4,7,10-tetraazacyclododecane-*N*,*N*′,*N*″,*N*‴-tetraacetic acid (DOTA) and then annealed this modified strand with the unmodified antisense strand for the determining biodistribution of siRNA in micellar carriers (*9*).

* Corresponding author. Naoto Oku, Department of Medical Biochemistry, University of Shizuoka School of Pharmaceutical Sciences, 52-1 Yada, Suruga-ku, Shizuoka 422-8526, Telephone number: +81-54-264-5701, Fax number: +81-54-264-5705, E-mail address: oku@u-shizuoka-ken.ac.jp.

[†] University of Shizuoka.

[‡] Hamamatsu Photonics K.K.

10.1021/bc9005267
Published on Web 03/08/2010

Viel et al. reported the conjugation of ^{18}F to oligonucleotide by using (*N*-[3-(2-[^{18}F]fluoropyridin-3-yloxy)-propyl]-2-bromoacetamide ([^{18}F]FRyBrA), and this method also required the annealing process (*10, 11*). In spite of their efforts, detail pharmacokinetic information about naked siRNA or siRNA in DDS carriers is still largely lacking.

In the present study, we developed a novel technique for labeling siRNA with a positron emitter, ^{18}F, in which double-stranded siRNA was labeled to gain conformational accuracy for examining the pharmacokinetics of siRNA by using [^{18}F]SFB as an ^{18}F labeling reagent. [^{18}F]SFB have been widely used to form a stable amide bond by reacting with primary amino groups for a short time and very easily for labeling certain peptides (*12*), antibodies (*13*), or DNA oligonucleotides (*14*). Because ^{18}F has an extremely short half-life (109 min), avoidance of the annealing process by labeling of double-stranded siRNA is favorable. [^{18}F]-labeled siRNA thus prepared was identified by ESI-TOF-MS, HPLC, and autoradiography after electrophoresis. By use of this positron emitter-labeled siRNA, we actually examined the biodistribution of siRNA by PPIS in the presence or absence of cationic liposome, a DDS carrier of siRNA. We also performed NIRF imaging for verifying the in vivo behavior of siRNA and discussed the correspondence of the imaging results obtained from NIRF imaging and PPIS imaging.

EXPERIMENTAL PROCEDURES

Materials. 4,7,13,16,21,24-Hexaoxa-1,10-diazabicyclo[8.8.8]-hexacosane (K[2.2.2]), tetra-*n*-propyl-ammonium hydroxide (Pr_4NOH), *N,N,N′,N′*-tetramethyl-*O*-(*N*-succinimidyl)uronium tetrafluoroborate (TSTU), CH_3CN (anhydrous), and fetal bovine serum were obtained from Sigma-Aldrich (Saint Louis, MO, USA). Potassium carbonate·$1.5H_2O$ was purchased from Merck (Darmstadt, Germany). Anion-exchange resin AG1-X8 (OH^- form, 100−200 mesh) was from Bio-Rad Laboratories (Hercules, USA). *N,N*-Dimethylformamide (DMF) was purchased from Wako Pure Chemical Industries, Ltd. (Osaka, Japan). A cationic lipid for transgene use, 1,2-dioleoyl-3-trimethylammonium-propane (DOTAP), was purchased from Avanti Polar Lipids Inc. (Alabaster, AL, USA). Cholesterol was kindly provided by Nippon Fine Chemical Co., Ltd. (Takasago, Hyogo, Japan). Trizol reagent was obtained from Invitrogen Co. (Carlsbad, CA). An alfalfa-free feed was purchased from Oriental Yeast co. Ltd. (Tokyo, Japan). Escain was purchased from Mylan Pharmaceuticals (Morgantown, WV). All other chemicals and solvents were analytical grade and were used without further purification unless otherwise stated. [^{18}F]Fluoride was produced with a cyclotron (HM-18, Sumitomo Heavy Industries, Tokyo, Japan) at Hamamatsu Photonics PET Center by the ^{18}O(p,n)^{18}F nuclear reaction using [^{18}O]H_2O. Labeled compounds were synthesized by using modified CUPID system (Sumitomo Heavy Industries, Tokyo, Japan). The HPLC column used for the purification of succinimidyl 4-[^{18}F] fluorobenzoate ([^{18}F]SFB) was an Inertsil ODS3 (10 × 250 mm, 5 μm, GL Sciences Inc., Tokyo, JAPAN). Nonradioactive fluorine-conjugated siRNA was identified by using a UPLC/ESI-QTOF-MS system, which consisted of an ACQUITY ultraperformance liquid chromatography (UPLC) system and an electrospray ionization quadrupole time-of-flight mass spectrometer (SYNAPT High Definition Mass Spectrometry system; Waters, Milford, MA, USA). An ultraviolet−visible (UV/vis) detector (ACQUITY TUV, Waters) was used. The UPLC column used for the identification of fluorine-labeled siRNA was an Acquity UPLC BEH C18 column (2.1 × 100 mm, 1.7 μm, Waters Corp.). The particle size and zeta-potential of nanoparticles were measured by using a Zetasizer Nano ZS (Malvern, Worcs, UK). Gel for obtaining an autoradiogram of ^{18}F and siRNA after electrophoresis was used an FLA-7000 (FUJIFILM Corporation, Tokyo, Japan) and LAS-3000 mini system (Fuji Film, Tokyo, Japan), respectively. Fluorescence imaging was performed by using a Xenogen IVIS Lumina System coupled to *Living Image* software for data acquisition (Xenogen Corp., Alameda, CA). PET imaging was performed by using a planar positron imaging system (PPIS, Hamamatsu Photonics, Shizuoka, Japan). Radioactivities in each organs were measured by gamma-counter (ARC-2000, Aloka, Tokyo, Japan).

Experimental Animals. Five-week-old male BALB/c mice male were purchased from Japan SLC Inc. (Shizuoka, Japan). The animals were cared for according to the Animal Facility Guidelines of the University of Shizuoka. All animal experiments were approved by the Animal and Ethics Review Committee of the University of Shizuoka.

siRNA Sequence. Alexa Fluor 750-labeled siRNA (AF750-siRNA) was purchased from Japan Bio Services Co., Ltd. (Saitama, Japan). Antisense strand contained a fluorescence at the 3′ end of the strand. siRNA for positron emitter-labeling was synthesized and purified by Hokkaido System Science. The nucleotide sequences of the siRNA were those of an unspecific scrambled RNA, and the antisense strand contained a 3′ amino C6 linker for the radioactive labeling of the siRNA duplex (Scheme 1). The sequences of the siRNA used were 5′-CGAUUCGCUAGACCGGCUUCAUUGCAG-3′ (sense) and 5′-GCAAUGAAGCCGGUCUAGCGAAUCGAU-3′ (antisense).

Synthesis of Ethyl-(4-Trimethylammonium)benzoate Trifluoromethanesulfonate. Ethyl 4-dimethylaminobenzoate was synthesized according to the procedure reported by Haka et al. (*15*). The synthetic compound was assigned by ^{1}H NMR and ^{13}C NMR. Ethyl 4-dimethylaminobenzoate 11.4 g (59 mmol) was dissolved in 70 mL anhydrous CH_2Cl_2. Ten grams of $CF_3SO_3CH_3$ (64.9 mmol) was added dropwise to the solution, and the mixture was stirred overnight at room temperature. A crystalline precipitate was formed by the addition of Et_2O (100 mL) and collected by suction filtration. Recrystallization from CH_2Cl_2/Et_2O gave 10.2 g (48%) of ethyl 4-trimethylammoniumbenzoate trifluoromethanesulfonate.

Radiosynthesis of [^{18}F]KF/K[2,2,2] Complex. [^{18}F]KF/K[2,2,2] was obtained by use of a previously reported method (*16*). In brief, [^{18}F]fluoride was trapped by ion-exchange resin AG1-X8 and eluted from the resin by 0.5 mL of 40 mM K_2CO_3. To this fluoride solution, 15 mg of K[2,2,2] in CH_3CN (2 mL) was added. Water was removed by azeotropic distillation at 110 °C under He flow (400 mL/min) for 5 min. To the residue, the addition of CH_3CN (1 mL) and azeotropic distillation were repeated twice. Then, the residue was dried under reduced pressure for 1 min, and the reaction vessel was purged with a flow of He (50 mL/min) for 1 min to ensure complete dryness. Finally, the reaction vessel was cooled to room temperature and used for further labeling.

Preparation of Succinimidyl 4-[^{18}F]fluorobenzoate ([^{18}F]-SFB). [^{18}F]SFB was prepared according to the one-pot procedure of Tang et al. (*17*) with some modifications. The precursor (5 mg) in 1.5 mL of CH_3CN was added to the dried [^{18}F]KF/K[2,2,2] complex mentioned above and reacted at 80 °C for 10 min. After the reaction mixture had been cooled, 20 μL of 1 M Pr_4NOH in 0.5 mL of CH_3CN was added; and hydrolysis was carried out at 120 °C for 5 min. Then, to the reaction mixture, TSTU (15 mg) in 0.5 mL of CH_3CN was added and converted to [^{18}F]SFB at 80 °C for 5 min. The reaction mixture was diluted with 2.0 mL of 5% CH_3COOH and transferred to the HPLC injector. Crude product was purified by semipreparative HPLC (CH_3CN:H_2O = 300:700, 6 mL/min, 254 nm). The radioactive peak eluted at 25.7 min was collected, diluted with 30 mL of H_2O, and passed through a Sep-Pak C18 cartridge (Waters). [^{18}F]SFB retained on the cartridge was released with 4 mL of CH_2Cl_2 and recovered into a V-vial by passage through a Sep-Pak Dry cartridge (Waters). Then, the [^{18}F]SFB was concen-

Scheme 1. Synthesis of the [^{18}F]SFB and [^{18}F]-Labeled siRNA

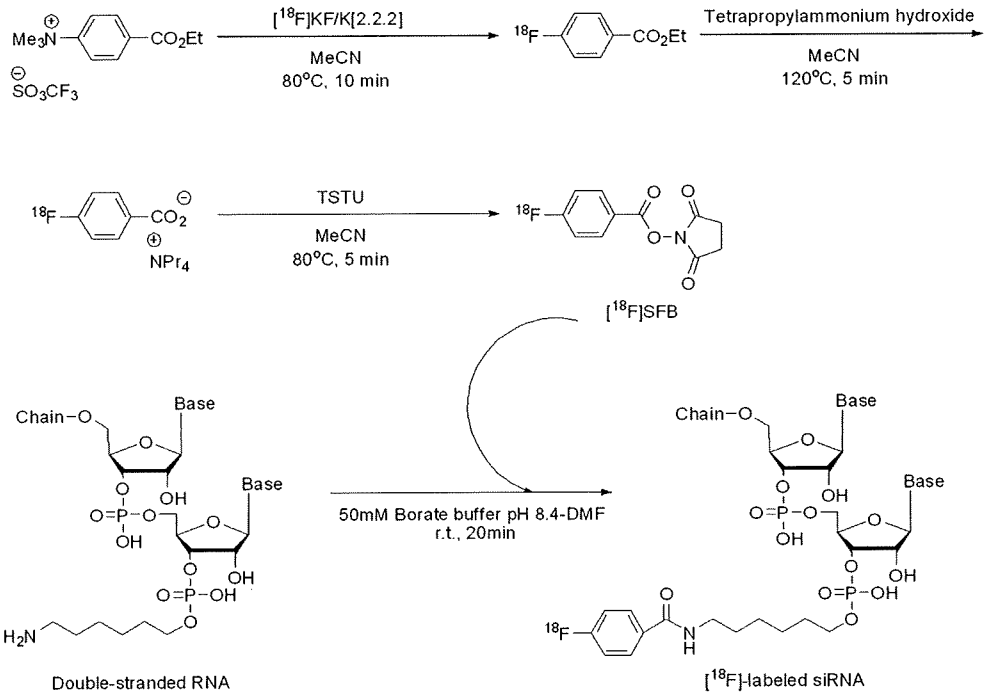

Table 1. Gradient Flow Table

time (min)	0.1 M TEAA (%)	CH_3CN (%)	flow rate (mL/min)
0–2	95–90	5–10	0.3
2–3	90–75	10–25	0.3
3–7	75–60	25–40	0.3
7–10	60–0	40–100	0.3

trated by a flow of He (200 mL/min) at 60 °C and used for labeling. [^{18}F]SFB with (a specific radioactivity of 51.4 GBq/μmol, a radiochemical yield of 21.1%) was obtained.

Radiolabeling of siRNA with [^{18}F]SFB. siRNA (40 nmol) in 16 μL of 50 mM borate buffer, pH 8.5, was added to the [^{18}F]SFB (60 nmol) in 3.6 μL of DMF. The mixture was vortexed for a few seconds and then incubated at room temperature for 20 min. The reaction mixture was purified and concentrated by ultrafiltration through a 10 000 molecular weight cutoff filter (Amicon, Millipore, Bedford, MA, USA). The mixture was centrifuged at 4000 × g with RNase-free phosphate-buffered saline (PBS). [^{18}F]-labeled siRNA with a radiochemical yield of 37.9% and a specific activity of 25.5 GBq/μmol was obtained. Nonradioactive fluorine-conjugated siRNA was synthesized in a similar manner except that 150 nmol cold SFB was used instead of 60 nmol [^{18}F]SFB.

Analytical Methods. Nonradioactive fluorine-conjugated siRNA was identified by using a UPLC/ESI-QTOF-MS system. The analytical column was maintained at 40 °C. A ultraviolet–visible (UV/vis) detector, equipped with a 500 nL flow cell, was also directly connected between the column outlet and the QTOF-MS instrument. Fractionation of fluorine-conjugated siRNA was performed at a flow rate of 0.3 mL/min using as the eluent the gradient of 0.1 M triethylammonium acetate (TEAA, pH 7.0) and CH_3CN. Gradient profile is presented in the Table 1.

Evaluation of siRNA Labeling. Precursor siRNA, fluorine-conjugated siRNA (non-RI), and [^{18}F]-labeled siRNA (0.5 μg) were applied to a 15% polyacrylamide gel and electrophoresed. Then, the gel was exposed to an imaging plate for obtaining an autoradiogram of ^{18}F by using an FLA-7000; the gel was stained for 5 min in ethidium bromide (EtBr), and siRNA was detected by using a LAS-3000 mini system.

Preparation of Cationic Liposomes and Their Complexes with siRNA. DOTAP and cholesterol (1:1 as a molar ratio) were dissolved in *tert*-butyl alcohol for freeze–drying and hydrated in RNase-free PBS. The liposomes were frozen and thawed for 3 cycles using liquid nitrogen and extruded 10 times through a polycarbonate membrane filter having a pore size of 100 nm (Nucleopore, Maidstone, UK). Then, the cationic liposome and siRNA were mixed gently and incubated for 10 min at room temperature to form liposome/siRNA complexes. The nitrogen moiety of cationic liposome to the phosphorus of siRNA (N/P ratio) was 24:1 in the complexes. The particle size and zeta-potential of liposome/siRNA complexes diluted with RNase-free PBS were measured. The particle size of liposome/siRNA complexes was 218 ± 3.0 nm (n = 3), and the particles showed monodispersion (polydispersity index = 0.16). The zeta-potential was 36.3 ± 1.9 mV.

Near-Infrared Fluorescence Imaging in Vivo. The biodistribution of AF750-siRNA was assessed by using an IVIS Lumina System. Mice were fed an alfalfa-free feed to reduce the effect of background fluorescence. The animals were anesthetized continuously via inhalation of 2% escain. siRNA or liposome/siRNA complexes containing 15 μg AF750-siRNA were injected via a tail vein under anesthesia. Alexa Fluor 750 fluorescence was acquired every 10 min for up to 60 min after the injection. After monitoring, the mice were sacrificed under anesthesia. Then, the organs, namely, heart, lungs, liver, spleen, and kidneys, were collected and imaged ex vivo with the IVIS.

PPIS Imaging of [^{18}F]-Labeled siRNA. Biodistribution of [^{18}F]-labeled siRNA was imaged noninvasively by using a PPIS (*18–20*). Animals were anesthetized with an intraperitoneal injection of pentobarbital at 50 mg/kg, and then fixed on an animal holder. To determine the whole-body biodistribution of siRNA, we administered the [^{18}F]-labeled siRNA intravenously (2.5 MBq/mouse). The scan was started immediately after the administration and performed for 60 min. Images were analyzed by using software *ImageJ*. After the PPIS scan, the mice were sacrificed for the collection of the blood from a carotid artery under anesthesia. Then, the heart, lungs, liver, spleen, and kidneys were removed, and the biodistribution of

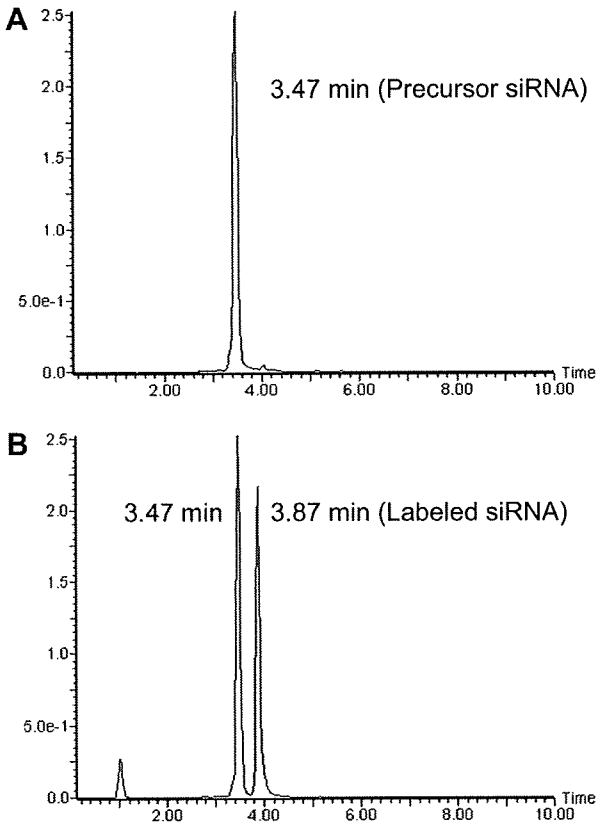

Figure 1. UPLC analysis of fluorine-conjugated siRNA. Nonradioactive fluorine was conjugated to siRNA and separated with the UPLC system. (A) Peak of precursor siRNA at 3.47 min. (B) Peaks of unreacted siRNA at 3.47 min and fluorine-labeled siRNA at 3.87 min after the reaction.

[^{18}F]-labeled siRNA was measured with a gamma counter. Distribution data were presented as percent dose per wet tissue. The total volume of blood was assumed to be 7.56% of the body weight. A time−activity curve was obtained from the mean pixel radioactivity in the region of interest (ROI) of the PPIS images.

Evaluation of siRNA Stability against Serum-Mediated Degradation. Fluorine-conjugated (0.5 μg) naked siRNA or that complexed with liposomes was incubated in 90% fetal bovine serum for 60 min at 37 °C. The siRNA was extracted from the serum by using Trizol reagent and subjected to 15% polyacrylamide gel electrophoresis. The gel was stained for 5 min in EtBr, and siRNA was detected by using a LAS-3000 mini system.

RESULTS

[^{18}F]-Labeling of siRNA and Its Radiochemistry. The methods for synthesis of [^{18}F]SFB and [^{18}F]-labeling of siRNA are shown in Scheme 1. At first, we prepared non-radioisotope (non-RI) fluorine-conjugated siRNA and identified the compound by using LC/ESI-TOF-MS (Table 1). Unreacted siRNA showed a peak at 3.47 min (Figure 1A). After the reaction, HPLC analysis indicated 2 main peaks, namely, labeled siRNA at 3.87 min and precursor siRNA at 3.47 min, respectively (Figure 1B). These peaks were fractionated by HPLC and analyzed by ESI-TOF-MS, giving multiply charged ion peaks of *m/z* $[M-8H]^{8-}$ 2196.1, $[M-7H]^{7-}$ 2510.9, and $[M-6H]^{6-}$ 2930.0 (data not shown), which corresponded to the labeled siRNA (expected mass of *m/z* $[M-8H]^{8-}$ 2196.7, $[M-7H]^{7-}$ 2510.7, and $[M-6H]^{6-}$ 2929.3). The overall yield of labeled siRNA was greater than 30% based on the peak area. On the basis of the result from non-RI fluorine-grafting to siRNA, [^{18}F]-labeled siRNA was prepared according to the same procedure, and then electrophoresis assay and subsequent autoradiography were performed to confirm the production of [^{18}F]-labeled siRNA. Electrophoresis assay with an imaging plate showed that the siRNA was labeled with [^{18}F]-fluorine without any other exposure bands (Figure 2). In addition, the main band visualized by EtBr staining showed the same position as the band on the same polyacrylamide gel observed by autoradiography. As a result, [^{18}F]-labeled siRNA was successfully prepared without any positron emitter-labeled byproducts, and the labeled siRNA was not degraded under the experimental conditions used.

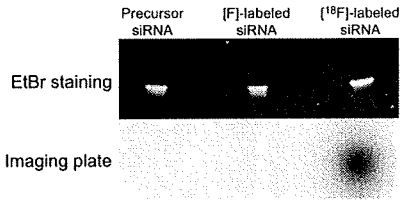

Figure 2. Demonstration of [^{18}F] labeling of siRNA. Precursor siRNA, fluorine-conjugated siRNA, and [^{18}F]-labeled siRNA were applied to a 15% polyacrylamide gel, electrophoresed, and stained with ethidium bromide. The gel was exposed to an imaging plate for detecting ^{18}F.

Biodistribution of siRNA Determined with near-Infrared Fluorescence Imaging in Vivo. We examined the in vivo behavior of siRNA by use of the NIRF imaging system. Mice were intravenously administered naked AF750-siRNA or liposome/AF750-siRNA complexes via a tail vein. The fluorescence imaging of AF750-siRNA was started immediately after the injection and monitored for 60 min. The biodistribution of AF750-siRNA is shown in Figure 3. The results indicated that the fluorescence compound was accumulated in the bladder immediately after the administration of naked AF750-siRNA and then excreted in the urine (Figure 3A). On the contrary, fluorescence was observed at the upper part of the body where the lung was positioned after the administration of liposome/AF750-siRNA complexes. The total fluorescence intensity of the image of mice injected with naked AF750-siRNA was apparently higher than that obtained with the liposomal formulation: Fluorescence in bladder after injection of naked siRNA was quite intense because bladder is located near the body surface, while that in lungs after injection of cationic liposome complexes was weak because lungs are located more deep from body surface compared with bladder.

The ex vivo imaging showed that a small amount of fluorescence remained in the kidneys but that no fluorescence was detected in the other tissues examined (Figure 3B). In contrast, the fluorescence of the cationic liposome/AF750-siRNA complexes accumulated in the lungs, being consistent with the in vivo imaging data.

Stability of Fluorine-Conjugated siRNA against Serum-Mediated Degradation. We evaluated the stability of naked fluorine-conjugated siRNA and cationic liposome/fluorine-conjugated siRNA complexes in serum for 60 min (Figure 4). The naked fluorine-conjugated siRNA incubated in PBS (control) was not decomposed. However, the band of naked siRNA obtained by electrophoresis of the sample that had been incubated in the presence of serum disappeared, indicating that the siRNA had been degraded by RNase within 60 min. In contrast, the band of siRNA was detected in the case of the cationic liposome/siRNA complexes exposed to the serum, indicating that complex formation protected siRNA from RNase in the serum.

In Vivo PPIS Imaging of siRNA Trafficking. Next, we examined [^{18}F]-labeled siRNA trafficking by use of PPIS. Mice were intravenously administered naked [^{18}F]-labeled siRNA in

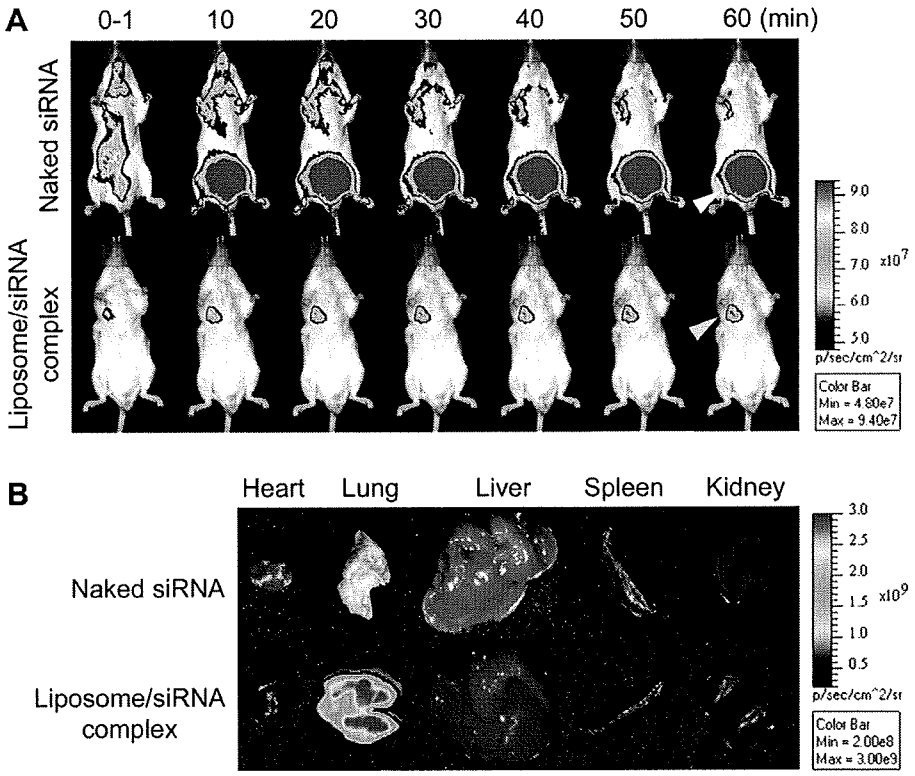

Figure 3. NIRF in vivo imaging with AF750-siRNA and liposome/AF750-siRNA complexes. (A) AF750- siRNA (top) or liposome/AF750-siRNA complexes (bottom) were intravenously administered to BALB/c mice. Images were acquired every 10 min for up to 60 min after the administration. The white arrowhead shows the bladder region, and the yellow arrowhead, the lung region. (B) Ex vivo imaging of AF750-siRNA and liposome/AF750-siRNA complexes at 60 min after administration.

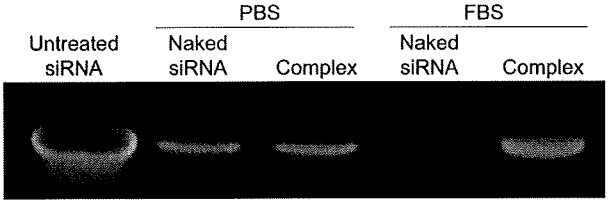

Figure 4. Stability of naked siRNA or liposome/siRNA complexes in FBS. siRNA (0.5 μg) was incubated with PBS (−) or 90% FBS at 37 °C for 60 min. siRNA was extracted and electrophoresed on a 15% polyacrylamide gel after a 60 min incubation and stained with EtBr. Untreated siRNA was used as a control marker.

PBS (−) or liposome/[^{18}F]-labeled siRNA complexes via a tail vein. The real-time imaging of [^{18}F]-labeled siRNA using PPIS was acquired for 60 min, and images were integrated every 5 min (Figure 5A). The ^{18}F radioactivity of the naked [^{18}F]-labeled siRNA accumulated inside the kidneys immediately after administration. This accumulation was not detected in NIRF in vivo imaging because of the influence of tissue depth. Then, ^{18}F was transferred to the bladder and subsequently excreted in the urine. In contrast, most of the ^{18}F radioactivity after the administration of cationic liposome/[^{18}F]-labeled siRNA complexes were retained in the lungs for 60 min, and only insignificant accumulation of them was observed in the bladder. The time−activity curve of ^{18}F in naked siRNA showed transient accumulation in kidney immediately after injection (19% injected dose/tissue at 2 min), and half of that was transferred to bladder at 21 min, and then the excretion of ^{18}F to bladder was gradually increased (Figure 5B). In contrast, the most of the ^{18}F after injection of liposome/siRNA complexes immediately accumulated in lungs and was maintained up to 60 min (76% injected dose/tissue). The biodistribution data obtained with a gamma counter after organ dissection showed that the ^{18}F after administration of naked [^{18}F]-labeled siRNA had not been distributed in any tissues tested, whereas the radioactivity after the injection of the cationic liposome/[^{18}F]-labeled siRNA complexes was highly distributed in the lungs (Figure 5C). These results corresponded roughly to the data obtained from the fluorescence ex vivo imaging.

Moreover, to confirm whether the accumulation of ^{18}F in the lungs after administration of cationic liposome/[^{18}F]-labeled siRNA reflected the accumulation of the liposomes of the complex, we examined the biodistribution of cationic liposome/siRNA complexes prepared with [^{3}H]cholesterylhexadecyl ether as a component. As a result, the liposomal complexes with siRNA were distributed in the lungs quite similarly to the distribution of the ^{18}F, suggesting that cationic liposome/siRNA accumulated in lungs as the complex form (Supporting Information Figure S1).

DISCUSSION

Recently, the topical application of siRNA medicines has reached clinical trial, and siRNA delivery systems for systemic injection have been extensively studied for the next generation of siRNA medicines (*21*). Pharmacokinetic information on siRNA molecules is considered to be particularly important for the acceleration of the development of siRNA medicine. Among the technologies for pharmacokinetic analysis, PET imaging technique is considered to be applicable to both preclinical trial and microdosing study (human phase 0 study). Using subtoxic and subpharmacologic doses, PET microdosing studies can be performed to screen for drug candidates for clinical trials on the basis of their pharmacokinetic properties (*22, 23*).

In the present study, we labeled double-stranded siRNA with^{18}F to obtain pharmacokinetics information about siRNA and siRNA in DDS carriers. We used [^{18}F]-fluorine as a short-

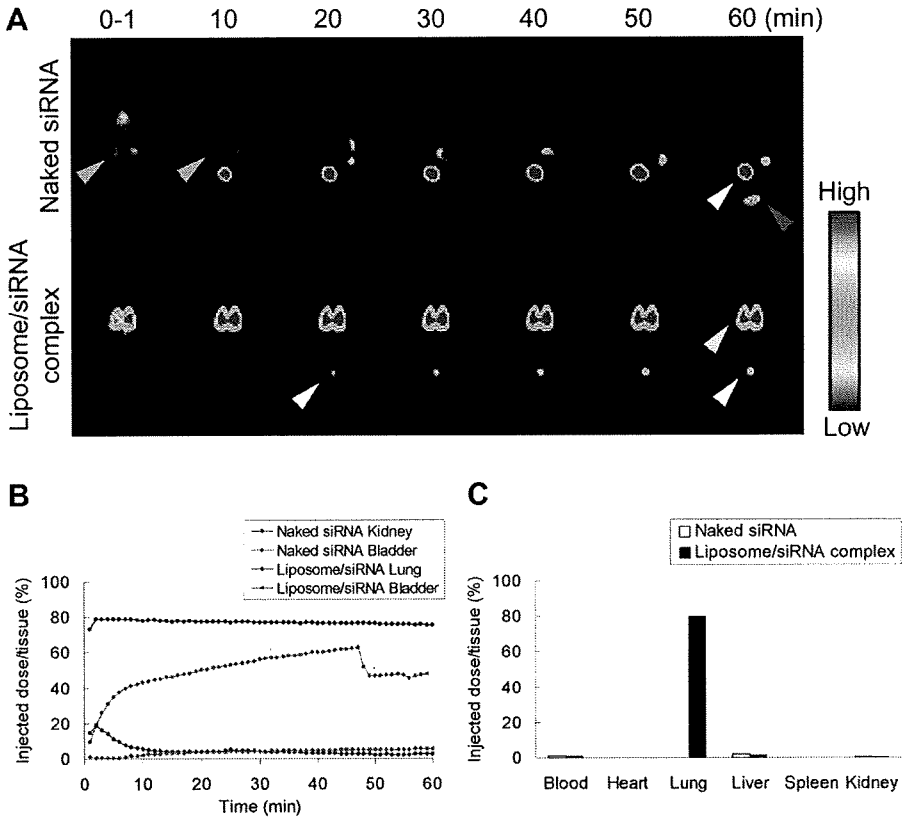

Figure 5. PPIS imaging with [^{18}F]-labeled siRNA and liposome/[^{18}F]-labeled siRNA complexes. (A) Naked siRNA (top) or liposome/siRNA complexes (bottom) at 2.5 MBq in 0.2 mL were intravenously administered to BALB/c mice. Images were acquired with a 1 min frame at 1, 10, 20, 30, 40, 50, and 60 min after the administration. The green arrowhead shows kidneys; the white one, the bladder; the red one, urine; and the yellow one, the lungs. (B) Real-time changes in [^{18}F]-labeled siRNA and liposomal [^{18}F]-labeled siRNA. Time activity curves of ^{18}F with naked siRNA shows kidney (blue) and bladder (red) and that of ^{18}F with cationic liposome/siRNA shows lung (black) and bladder (green). (C) After the PPIS scan, the mice were sacrificed, and biodistribution of ^{18}F in each organ was then measured with a gamma counter.

lived positron-emitting radionuclide (half-life: 109 min), which has been applied to humans for cancer diagnosis in the form of [2-^{18}F]2-deoxy-2-fluoroglucose ([^{18}F]FDG). The advantages of the present methodology to label siRNA are that (1) the modification of double-stranded RNA with amino group enables fast preparation and purification without the time-consuming process of annealing and (2) the methodology maintains the conformational accuracy of the siRNA. Indeed, reaction of siRNA and [^{18}F]SFB was complete within 20 min. In addition, fluorine-conjugated siRNA was identified by LC and ESI-TOF-MS (Figure 1) and did not decompose during the reaction or purification process (Figure 2).

It is well-known that one of the most important factors regarding the biodistribution of liposomes in vivo is the charge of the liposomal surface. Positively charged complexes aggregate in the presence of serum proteins (*24*), are entrapped in the lung capillaries, and thus accumulate in the lung tissue (*25, 26*) after intravenous administration. In fact, when liposomes were labeled with [^{3}H]cholesterylhexadecyl ether, the radioactivity of cationic liposome/siRNA complexes accumulated in the lungs (Supporting Information Figure S1). However, since nucleic acids such as siRNAs and oligodeoxynucleotides (ODNs) are known to be eliminated from the circulation via the kidneys and excreted into the urine 60 min after administration via a tail vein (*27, 28*), distribution studies on siRNAs or ODNs besides on their carriers are important for the development of nucleic acid medicines. In the distribution study, [^{3}H]cholesterylhexadecyl ether was accumulated in the liver to some extent, although the accumulation of siRNA was not observed after injection of cationic liposome/siRNA complex. We speculate that siRNA was degraded in the liver and excreted, while cholesterylhexadecyl ether did not.

In the present study, we first used AF750-siRNA and examined its in vivo behavior by using NIRF fluorescence imaging. NIRF fluorescence was rapidly cleared from the bloodstream and excreted in the bladder after the administration of naked AF750-siRNA (Figure 3). In contrast, the fluorescence of cationic liposome/siRNA complexes accumulated in the lungs. However, the differential fluorescence intensities between in vivo images and ex vivo ones indicated the limitation of NIRF imaging. Quantitative analysis could not be applied due to the influence of tissue depth on the fluorescence intensity. Moreover, it is possible that fluorescence self-quenching and/or resonance energy transfer affect the intensity.

In contrast to NIRF imaging, PPIS or PET technology provides quantitative analytic data with high spatial resolution. ^{18}F was observed in the kidneys until 10 min after the administration of naked [^{18}F]-labeled siRNA, and subsequently, it was transferred to the bladder and excreted into urine (Figure 5). This result is consistent with previous result reported by Viel et al. who used ^{18}F-labeled naked siRNA (*11*). Other reports also presented the renal excretion of siRNA (*27, 29, 30*). In addition, Bartlett et al. reported that the excretion of ^{64}Cu-labeled naked siRNA was quite fast (*9*). They indicated that the siRNA in a complex with cyclodextrin-containing polycation excreted quite rapidly and suggested the instability of the complex. Therefore, determination of siRNA trafficking instead of carrier trafficking is important for the development of siRNA medicines. In contrast to the in vivo fate of naked siRNA, the ^{18}F of

cationic liposome/[^{18}F]-labeled siRNA complexes was spread throughout the lungs and was retained in them at least up to 60 min.

Next, we investigated the stability of siRNA in the presence of serum by performing an electrophoresis assay. The data indicated that naked siRNA was degraded when incubated for 60 min in serum, whereas the liposome/siRNA complexes were not (Figure 4). These results suggest that naked siRNA has a short half-life in vivo and is rapidly eliminated by renal excretion as a degraded form. However, further study is needed to clarify whether the excreted siRNA is in the intact form or degraded form. On the other hand, a part of the ^{18}F showed enterohepatic circulation. This enterohepatic circulation would be mediated by some of the fragmented siRNA having the polar moiety (the alkyl chain on the 3′ end of the antisense strand) and nonpolar moiety (siRNA).

As indicated above, the serum stability study showed that the liposomal siRNA was not degraded in the presence of serum. Furthermore, the ^{18}F distribution of liposomal [^{18}F]-labeled siRNA was similar to the distribution of the [^{3}H]-labeled liposome carrier: Both were accumulated in the lungs after intravenous administration. Taken together, our data strongly suggest that liposomal siRNA would be delivered to the lungs in its intact form. In conclusion, we developed a novel positron emitter-labeling methodology for siRNA and evaluated the in vivo trafficking of [^{18}F]-labeled siRNA by PPIS. The results of present study suggest that siRNA is stable as a complex with liposomes and should be deliverable specific tissues depending on the characteristics of the carrier. Therefore, designing the DDS carrier expands the usefulness of siRNA in vivo, and the present technology might support the development of siRNA medicines.

ACKNOWLEDGMENT

This study was financially supported by the Health and Labor Sciences Research Grants from the Ministry of Health, Labour, and Welfare of Japan. Synthesis of positron emitter-labeled siRNA was supported in part by Hokkaido System Science Co. Ltd. We thank Drs. T. Kakiuchi and H. Uchida at Hamamatsu Photonics K.K. PET Center for PET study for their technical assistance. They also thank Drs. S. Akai and T. Toyo'oka at the University Shizuoka for their valuable discussions as well as for allowing us to use their facilities. We also acknowledge Dr. S. Inagaki for helpful discussions and excellent technical assistance.

Supporting Information Available: Preparation of [^{3}H]-labeled liposome and complex. Biodistribution of liposomes and complexes. This material is available free of charge via the Internet at http://pubs.acs.org.

LITERATURE CITED

(1) Fire, A., Xu, S., Montgomery, M. K., Kostas, S. A., Driver, S. E., and Mello, C. C. (1998) Potent and specific genetic interference by double-stranded RNA in Caenorhabditis elegans. *Nature 391*, 806–811.

(2) Elbashir, S. M., Harborth, J., Lendeckel, W., Yalcin, A., Weber, K., and Tuschl, T. (2001) Duplexes of 21-nucleotide RNAs mediate RNA interference in cultured mammalian cells. *Nature 411*, 494–498.

(3) Pai, S. I., Lin, Y. Y., Macaes, B., Meneshian, A., Hung, C. F., and Wu, T. C. (2006) Prospects of RNA interference therapy for cancer. *Gene Ther. 13*, 464–477.

(4) Jeong, J. H., Mok, H., Oh, Y. K., and Park, T. G. (2009) siRNA conjugate delivery systems. *Bioconjugate Chem. 20*, 5–14.

(5) Zimmermann, T. S., Lee, A. C. H., Akinc, A., Bramlage, B., Bumcrot, D., Fedoruk, M. N., Harborth, J., Heyes, J. A., Jeffs, L. B., John, M., Judge, A. D., Lam, K., McClintock, K., Nechev, L. V., Palmer, L. R., Racie, T., Rohl, I., Seiffert, S., Shanmugam, S., Sood, V., Soutschek, J., Toudjarska, I., Wheat, A. J., Yaworski, E., Zedalis, W., Koteliansky, V., Manoharan, M., Vornlocher, H. P., and MacLachlan, I. (2006) RNAi-mediated gene silencing in non-human primates. *Nature 441*, 111–114.

(6) Kim, S. H., Jeong, J. H., Lee, S. H., Kim, S. W., and Park, T. G. (2008) LHRH receptor-mediated delivery of siRNA using polyelectrolyte complex micelles self-assembled from siRNA-PEG-LHRH conjugate and PEI. *Bioconjugate Chem. 19*, 2156–2162.

(7) Medarova, Z., Pham, W., Farrar, C., Petkova, V., and Moore, A. (2007) In vivo imaging of siRNA delivery and silencing in tumors. *Nat. Med. 13*, 372–377.

(8) Urakami, T., Akai, S., Katayama, Y., Harada, N., Tsukada, H., and Oku, N. (2007) Novel amphiphilic probes for [^{18}F]-radiolabeling preformed liposomes and determination of liposomal trafficking by positron emission tomography. *J. Med. Chem. 50*, 6454–6457.

(9) Bartlett, D. W., Su, H., Hildebrandt, I. J., Weber, W. A., and Davis, M. E. (2007) Impact of tumor-specific targeting on the biodistribution and efficacy of siRNA nanoparticles measured by multimodality *in vivo* imaging. *Proc. Natl. Acad. Sci. U.S.A. 104*, 15549–15554.

(10) Viel, T., Kuhnast, B., Hinnen, F., Boisgard, R., Tavitian, B., and Dolle, F. (2007) Fluorine-18 labelling of small interfering RNAs (siRNAs) for PET imaging. *J. Labelled Compd. Radiopharm. 50*, 1159–1168.

(11) Viel, T., Boisgard, R., Kuhnast, B., Jego, B., Siquier-Pernet, K., Hinnen, F., Dolle, F., and Tavitian, B. (2008) Molecular imaging study on *in vivo* distribution and pharmacokinetics of modified small interfering RNAs (siRNAs). *Oligonucleotides 18*, 201–212.

(12) Chen, X., Park, R., Shahinian, A. H., Tohme, M., Khankaldyyan, V., Bozorgzadeh, M. H., Bading, J. R., Moats, R., Laug, W. E., and Conti, P. S. (2004) 18F-labeled RGD peptide: initial evaluation for imaging brain tumor angiogenesis. *Nucl. Med. Biol. 31*, 179–189.

(13) Vaidyanathan, G., and Zalutsky, M. R. (1994) Improved synthesis of N-succinimidyl 4-[^{18}F]fluorobenzoate and its application to the labeling of a monoclonal-antibody fragment. *Bioconjugate Chem. 5*, 352–356.

(14) Li, J., Trent, J. O., Bates, P. J., and Ng, C. K. (2006) Labeling G-rich oligonucleotides (GROs) with N-succinimidyl 4-[^{18}F]fluorobenzoate (S18FB). *J. Labelled Compd. Radiopharm. 49*, 1213–1221.

(15) Haka, M. S., Kilbourn, M. R., Watkins, G. L., and Toorongian, S. A. (1989) Aryltrimethylammonium trifluoromethanesulfonates as precursors to aryl [^{18}F] fluorides: improved synthesis of [^{18}F] GBR-13119. *J. Labelled Compd. Radiopharm. 27*, 823–833.

(16) Harada, N., Ohba, H., Fukumoto, D., Kakiuchi, T., and Tsukada, H. (2004) Potential of [^{18}F]β-CFT-FE (2β-carbomethoxy-3β-(4-fluorophenyl)-8-(2-[^{18}F]fluoroethyl)nortropane) as a dopamine transporter ligand: A PET study in the conscious monkey brain. *Synapse 54*, 37–45.

(17) Tang, G., Zeng, W. B., Yu, M. X., and Kabalka, G. (2008) Facile synthesis of N-succinimidyl 4-[^{18}F]fluorobenzoate ([^{18}F]SFB) for protein labeling. *J. Labelled Compd. Radiopharm. 51*, 68–71.

(18) Takamatsu, H., Kakiuchi, T., Noda, A., Uchida, H., Nishiyama, S., Ichise, R., Iwashita, A., Mihara, K., Yamazaki, S., Matsuoka, N., Tsukada, H., and Nishimura, S. (2004) An application of a new planar positron imaging system (PPIS) in a small animal: MPTP-induced parkinsonism in mouse. *Ann. Nucl. Med. 18*, 427–431.

(19) Uchida, H., Okamoto, T., Ohmura, T., Shimizu, K., Satoh, N., Koike, T., and Yamashita, T. (2004) A compact planar positron imaging system. *Nucl. Instrum. Methods Phys. Res., Sect. A 516*, 564–574.

(20) Uchida, H., Sato, K., Kakiuchi, T., Fukumoto, D., and Tsukada, H. (2008) Feasibility study of quantitative radioactivity monitoring of tumor tissues inoculated into mice with a planar positron imaging system (PPIS). *Ann. Nucl. Med. 22*, 57–63.

(21) de Fougerolles, A. R. (2008) Delivery vehicles for small interfering RNA *in vivo*. *Hum. Gene Ther. 19*, 125–32.

(22) Bauer, M., Wagner, C. C., and Langer, O. (2008) Microdosing studies in humans: the role of positron emission tomography. *Drugs in R&D 9*, 73–81.

(23) Wagner, C. C., Muller, M., Lappin, G., and Langer, O. (2008) Positron emission tomography for use in microdosing studies. *Curr. Opin. Drug Discovery Dev. 11*, 104–110.

(24) Litzinger, D. C., Brown, J. M., Wala, I., Kaufman, S. A., Van, G. Y., Farrell, C. L., and Collins, D. (1996) Fate of cationic liposomes and their complex with oligonucleotide *in vivo*. *Biochim. Biophys. Acta, Biomembr. 1281*, 139–149.

(25) Li, S., Tseng, W. C., Stolz, D. B., Wu, S. P., Watkins, S. C., and Huang, L. (1999) Dynamic changes in the characteristics of cationic lipidic vectors after exposure to mouse serum: implications for intravenous lipofection. *Gene Ther. 6*, 585–594.

(26) McLean, J. W., Fox, E. A., Baluk, P., Bolton, P. B., Haskell, A., Pearlman, R., Thurston, G., Umemoto, E. Y., and McDonald, D. M. (1997) Organ-specific endothelial cell uptake of cationic liposome-DNA complexes in mice. *Am. J. Physiol. 273*, H387–404.

(27) van de Water, F. M., Boerman, O. C., Wouterse, A. C., Peters, J. G., Russel, F. G., and Masereeuw, R. (2006) Intravenously administered short interfering RNA accumulates in the kidney and selectively suppresses gene function in renal proximal tubules. *Drug Metab. Dispos. 34*, 1393–1397.

(28) Lendvai, G., Velikyan, I., Bergstrom, M., Estrada, S., Laryea, D., Valila, M., Salomaki, S., Langstrom, B., and Roivainen, A. (2005) Biodistribution of 68Ga-labelled phosphodiester, phosphorothioate, and 2′-O-methyl phosphodiester oligonucleotides in normal rats. *Eur. J. Pharm. Sci. 26*, 26–38.

(29) Braasch, D. A., Paroo, Z., Constantinescu, A., Ren, G., Oz, O. K., Mason, R. P., and Corey, D. R. (2004) Biodistribution of phosphodiester and phosphorothioate siRNA. *Bioorg. Med. Chem. Lett. 14*, 1139–1143.

(30) Liu, N., Ding, H., Vanderheyden, J. L., Zhu, Z., and Zhang, Y. (2007) Radiolabeling small RNA with technetium-99m for visualizing cellular delivery and mouse biodistribution. *Nucl. Med. Biol. 34*, 399–404.

BC9005267

International Journal of Pharmaceutics 392 (2010) 218–223

Contents lists available at ScienceDirect

International Journal of Pharmaceutics

journal homepage: www.elsevier.com/locate/ijpharm

Pharmaceutical Nanotechnology

T cell-independent B cell response is responsible for ABC phenomenon induced by repeated injection of PEGylated liposomes

Hiroyuki Koide[a], Tomohiro Asai[a], Kentaro Hatanaka[a], Shuji Akai[b], Takayuki Ishii[a], Eriya Kenjo[a], Tatsuhiro Ishida[c], Hiroshi Kiwada[c], Hideo Tsukada[d], Naoto Oku[a,*]

[a] Department of Medical Biochemistry and Global COE Program, Graduate School of Pharmaceutical Sciences, University of Shizuoka, 52-1 Yada, Suruga-ku, Shizuoka 422-8526, Japan
[b] Department of Synthetic Organic Chemistry, Graduate School of Pharmaceutical Sciences, University of Shizuoka, 52-1 Yada, Suruga-ku, Shizuoka 422-8526, Japan
[c] Department of Pharmacokinetics and Biopharmaceutics, Institute of Health Biosciences, The University of Tokushima, 1-78-1, Sho-machi, Tokushima 770-8505, Japan
[d] Central Research Laboratory, Hamamatsu Photonics K.K., Hamamatsu, Shizuoka, Japan

ARTICLE INFO

Article history:
Received 9 December 2009
Received in revised form 8 February 2010
Accepted 8 March 2010
Available online 21 March 2010

Keywords:
Polyethylene glycol
Liposome
Accelerated blood clearance
Thymus-independent type 2 antigen
Nanocarriers

ABSTRACT

Repeated injection of polyethyleneglycol-modified (PEGylated) liposomes causes a rapid clearance of them from the bloodstream, this phenomenon is called accelerated blood clearance (ABC). In the present study, we focused on the immune system responsible for the ABC phenomenon. PEGylated liposomes were preadministered to BALB/c mice and [^{3}H]-labeled ones were then administered to them 3 days after the preadministration. Consistent with our previous results, the preadministration with PEGylated liposomes triggered the rapid clearance of [^{3}H]-labeled PEGylated liposomes from the bloodstream, but that with PEGylated liposomes encapsulating doxorubicin (Dox) did not. In addition, we found that the ABC phenomenon was observed when a mixture of free Dox and PEGylated liposomes was preadministered. These data indicate that immune cells responsible for the ABC phenomenon might be selectively damaged by the Dox encapsulated in PEGylated liposomes. The ABC phenomenon was also observed in BALB/c *nu/nu* mice, but not in BALB/c SCID mice. The amount of anti-PEG IgM antibody induced by the stimulation with the PEGylated liposomes was significantly increased in the BALB/c *nu/nu* mice, but not in the BALB/c SCID ones. These data indicate that a T cell-independent B cell response would play a significant role in the ABC phenomenon. Furthermore, the present study suggests that PEGylated liposomes might be recognized by B cells as a thymus-independent type 2 (TI-2) antigen. The present study provides important information for the future development of liposomal medicines.

1. Introduction

PEGylated liposomes have been widely investigated as drug carriers and gene delivery systems. PEG forms a water shell on the liposomal surface and provides a steric barrier to the liposomes for avoiding interactions with plasma proteins, resulting in escape from trapping by the reticuloendothelial system (Lasic et al., 1991; Torchilin et al., 1994; Van Rooijen and Van Nieuwmegen, 1980). Therefore, PEGylated liposomes have the property of long circulation and are useful for drug delivery to tumors and inflamed sites, resulting in improving the therapeutic indices of encapsulated drugs (Allen, 1994). As a representative example of liposomal drugs, Doxil® has been used clinically. Doxil® is PEGylated liposomes encapsulating doxorubicin, which is used for reducing side effects of Dox such as cardiotoxicity and for enhancing its anticancer activity through enhanced permeability and retention (EPR) effect (Berry et al., 1998; Maeda et al., 2000; Muggia, 1999). On the other hand, we and others have found that a repeat injection of PEGylated liposomes into certain animals such as mice, rats and rhesus monkey triggers the rapid clearance of the second dose through their accumulation in the liver (Dams et al., 2000; Ishida et al., 2003a,b). This phenomenon, called as the accelerated blood clearance (ABC) phenomenon, is expected to have a considerable impact on the clinical use of liposomal formulations (Dams et al., 2000; Ishida et al., 2003a,b). A previous study of ours indicated that when rats were pretreated with a high dose (more than 5 μmol phospholipids/kg) of PEGylated liposomes, the induction of the ABC phenomenon was weakened. However, when rats were pretreated with a low concentration of them (1 μmol phospholipids/kg), the phenomenon was strongly induced (Ishida et al., 2006a,b,c). This phenomenon was widely observed even if the content of PEG lipid in liposomes or the length of the

Abbreviations: ABC phenomenon, accelerated blood clearance phenomenon; [^{3}H]-CHE, [^{3}H] cholesterylhexadecyl ether; MPEG-DSPE, 1,2-distearoyl-sn-glycero-3-phosphoethanolamine-n-[methoxy(polyethylene glycol)-2000]; MPS, mononuclear phagocyte system; PEGylated liposomes, polyethylene glycol-modified liposomes.

* Corresponding author. Tel.: +81 54 264 5701; fax: +81 54 264 5705.
E-mail address: oku@u-shizuoka-ken.ac.jp (N. Oku).

0378-5173/$ – see front matter © 2010 Elsevier B.V. All rights reserved.
doi:10.1016/j.ijpharm.2010.03.022

PEG chain was varied. In fact, both methoxy(polyethyleneglycol)-2000-distearoylphosphatidylethanolamine ($mPEG_{2000}$-DSPE) and $mPEG_{5000}$-DSPE induced the phenomenon, and the concentration of $mPEG_{2000}$-DSPE in the first-dose PEGylated liposomes did not affect on the induction of the phenomenon (Ishida et al., 2005). In an earlier study, we also demonstrated that the spleen could play a key role in induction of the ABC phenomenon via secretion of anti-PEG IgM antibody by splenic B cells (Ishida et al., 2006a,b,c). Anti-PEG IgM antibody was gradually secreted by the administration of PEGylated liposomes and bound to the liposomes in the secondary injection, resulting in the rapid clearance of them from the bloodstream via complement activation (Ishida et al., 2005, 2007). Furthermore, the ABC phenomenon was triggered by preadministration with not only PEGylated liposomes but also polymeric micelles having PEG chains (Koide et al., 2008).

Our recent reports showed that the administration of Dox encapsulated in PEGylated liposomes (PEG–Dox) did not alter the pharmacokinetics of PEGylated liposomes injected as the test-dose (Ishida et al., 2006a,b,c; Laverman et al., 2001). In the present study, we firstly focused on the effect of Dox in the liposomes on the immune cells responsible for the ABC phenomenon. Then, we investigated the immune mechanism involved in this phenomenon.

2. Materials and methods

2.1. Materials

Dipalmitoylphosphatidylcholine (DPPC), cholesterol (Cho), and distearoylphosphoethanolamine-*N*-[methoxy(polyethyleneglycol)-2000] (mMPEG-DSPE) were kindly donated by Nippon Fine Chemical Co., Ltd. (Takasago, Hyogo, Japan). [^{3}H]cholesterylhexadecyl ether ([^{3}H]-CHE) was purchased from Amersham Pharmacia (Buckinghamshire, UK). All other reagents were analytical grade.

2.2. Animal

Five-week-old male BALB/c and BALB/c *nu/nu* mice were purchased from Japan SLC Inc. (Shizuoka, Japan). Five-week-old male CB17/Icr-Prkdc^{scid}/CrlCrlj (BALB/c SCID) mice were purchased from Charles River Japan, Inc. (Kanagawa, Japan). The animals were cared according to the animal facility guidelines of the University of Shizuoka.

2.3. Preparation of liposomes

PEGylated liposomes composed of DPPC and Cho with mPEG-DSPE (10:5:1 as a molar ratio) were prepared as described previously (Maeda et al., 2004). In brief, lipids dissolved in chloroform were evaporated to obtain a thin lipid film. Then, liposomes were formed by hydration with 10 mM phosphate-buffered 0.3 M sucrose solution and then sized by 5-times extrusion through a polycarbonate membrane filter with 100 nm pores (Nucleopore, Maidstone, UK). For a biodistribution study, a trace amount of [^{3}H]-CHE (74 kBq/mouse) was added to the initial chloroform solution. Dox-encapsulated liposomes were prepared by a modification of the remote loading method as described previously (Oku et al., 1994). The concentration of Dox was determined by its absorbance at 484 nm. The particle size of PEGylated liposomes was measured by use of a Zetasizer Nano ZS (MALVERN, Worcestershire, UK) after dilution of the liposomes with PBS, pH 7.4.

2.4. Biodistribution of PEGylated liposomes

Mice received an intravenous injection of PEGylated liposomes (2.0 μmol phospholipids/kg), PEG–Dox liposomes (1 mg/kg as a Dox dosage), a mixture of free Dox (1 mg/kg) and "empty" PEGylated liposomes or PBS. Three days later, [^{3}H]-labeled PEGylated liposomes (5.0 μmol phospholipids/kg) were administered to the mice via a tail vein. Twenty-four hours after the second administration, these mice were sacrificed under deep anesthesia for the collection of blood. Then, the blood was heparinized and separated by centrifugation (700 × *g*, 15 min, 4 °C) to obtain the plasma. After the mice had been bled from the carotid artery, their heart, lungs, liver, spleen, and kidneys were removed and weighed. The radioactivity in plasma and each organ was determined with a liquid scintillation counter (LSC-3100, Aloka, Tokyo, Japan). Tissue distribution data were presented as % dose per wet tissue. The total radioactivity in the plasma was calculated based on the average body weight of the mice, where the average plasma volume was assumed to be 4.27% of the body weight based on the data on total blood volume.

2.5. Detection of anti-PEG IgM antibody

Mice were intravenously injected with PEGylated liposomes (2.0 μmol phospholipids/kg), PEG–Dox liposomes (1 mg/kg as a Dox dosage), a mixture of free Dox (1 mg/kg) and "empty" PEGylated liposomes or PBS. Three days later, these mice were sacrificed and their blood was withdrawn. Serum was collected after centrifugation (700 × *g*, 15 min, 4 °C). To prepare the ELISA plates, 10 μg of mPEG-DSPE in 20 μL ethanol was added to 96-well plates (Nunc, Roskilde, Denmark). Then, the plates were air dried for 2 h to complete dryness and subsequently blocked with 10% fetal bovine serum (FBS, Sigma–Aldrich, St. Louis, MO) in PBS for 1 h. The diluted serum samples (100 μl) were added to the plates, incubated for 1 h, and washed 5 times with 1% FBS-PBS. Antibodies bound to mPEG-DSPE were detected with HRP-conjugated goat anti-mouse IgM antibody (Bethyl Laboratories, TX, USA). After incubation with the anti-IgM antibody for 1 h, each well was washed 5 times with 1% FBS-PBS. The coloration was initiated by the addition of *o*-phenylene diamine dihydrochloride (Sigma, St. Louis, MO, USA) that had been diluted with distilled water. After a 15-min incubation, the reaction was stopped by adding 100 μL of 2 M H_2SO_4, and the absorbance was recorded at 490 nm.

2.6. Synthesis of a positron emitter-labeled probe

The synthesis of 1-[^{18}F] fluoro-3,6-dioxatetracosane (SteP2) was prepared as described previously (Urakami et al., 2007). Briefly, [^{18}F] fluoride was produced with a cyclotron (HM-18, Sumitomo Heavy Industries, Tokyo, Japan) at Hamamatsu Photonics PET Center, and the labeled compound was synthesized from the precursor.

2.7. [^{18}F]-Labeling of PEGylated liposomes

[^{18}F]-Labeling of PEGylated liposomes were performed by a solid-phase transition (SophT) method (Urakami et al., 2007). About 100 MBq of [^{18}F]-SteP2 in ethanol solution was transferred to a glass test tube, and the solvent was removed completely at 90 °C with a flow of helium gas. PEGylated liposomes were added to the tube and incubated at 37 °C for 15 min with 5-s mixing by use of a vortex stirrer every 3 min. After the incubation, the PEGylated liposomes were centrifuged at 100,000 × *g* for 15 min (Beckman, Fullerton, CA, USA), and the supernatant was transferred to a new tube. Radioactivity of supernatant, precipitate, and original tube for labeling was measured with a curiemeter (IGC-3, Aloka, Tokyo, Japan) to calculate the labeling efficiency.

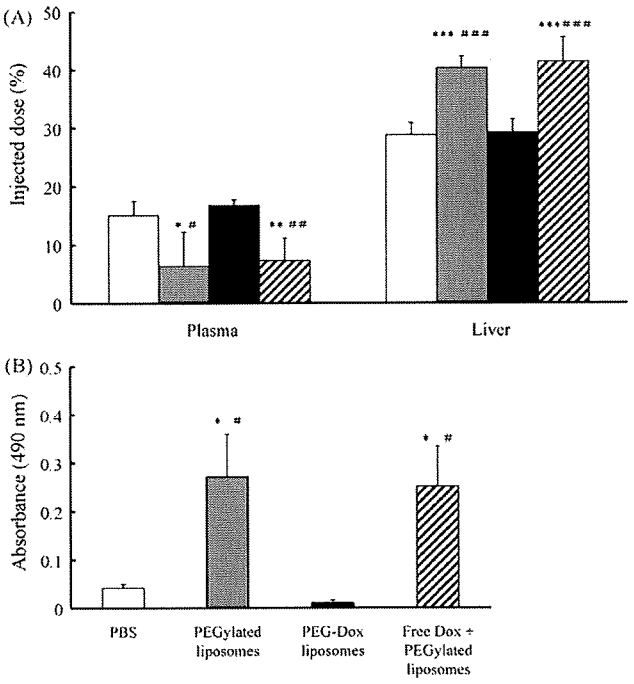

Fig. 1. Abolishment of the ABC phenomenon with Dox encapsulated in PEGylated liposomes. BALB/c mice were intravenously injected with PBS, PEGylated liposomes, PEG–Dox liposomes or a mixture of free Dox and "empty" PEGylated liposomes. (A) Biodistribution of the test-dose ^{3}H-labeled PEGylated liposomes: 3 days after the pretreatment, ^{3}H-labeled PEGylated liposomes were intravenously injected into these mice (5 μmol DPPC dosage/kg). Twenty-four hours after the second injection, the mice were sacrificed, and the radioactivity in the plasma and each organ (only liver data shown) was determined. Data ($n = 5$) are presented as a percentage of the injected dose per tissue and S.D. and (B) anti-PEG IgM in the serum collected at day 3 after the pretreatment. Each value represents the mean ± S.D. of 3 separate experiments. Data are presented for PBS (open bar), PEGylated liposomes (gray bar), PEG–Dox liposomes (closed bar), and a mixture of free Dox and PEGylated liposomes (hatched bar). Significant differences: $^{*}p < 0.05$, $^{**}p < 0.01$, and $^{***}p < 0.001$ *vs.* PBS; $^{\#}p < 0.05$, $^{\#\#}p < 0.01$, and $^{\#\#\#}p < 0.001$ *vs.* PEG–Dox.

2.8. Imaging of [^{18}F]-labeled PEGylated liposomes by planar positron imaging system (PPIS)

Biodistribution of [^{18}F]-labeled PEGylated liposomes was determined with a positron planar imaging system (PPIS, Hamamatsu Photonics, Shizuoka, Japan). Mice anesthetized with chloral hydrate were positioned prone on an acrylic plate and placed between the 2 opposing detectors. An [^{18}F]-labeled sample at the dose of 2.5 MBq was intravenously injected into a mouse via a tail vein. The data were acquired with a 1-min time frame interval for 60 min, and 2 summation images were created every 30 min.

2.9. Statistics

Variance in a group was evaluated by using Student's *t*-test.

3. Results

3.1. Abolishment of ABC phenomenon by preadministration with Dox encapsulated in PEGylated liposomes

Mice were intravenously injected with PEGylated liposomes, PEG–Dox liposomes, a mixture of free Dox and "empty" PEGylated liposomes, or PBS for preconditioning. Three days later, these mice were administered PEGylated liposomes labeled with [^{3}H]-CHE as the test-dose. Fig. 1A shows the biodistribution of the test-dose PEGylated liposomes 24 h after the injection. Pretreatment with the PEG–Dox liposomes did not alter the plasma level or hepatic uptake of the test-dose compared with that with PBS. However, in case of pretreatment with the mixture of free Dox and "empty" PEGylated liposomes, the amount of test-dose significantly decreased in the plasma and significantly increased in the liver. The biodistribution pattern for this group was similar to that for the PEGylated liposome-injected group. The accumulation of the test-dose in other organs did not show significant differences among all groups tested (data not shown). Next, anti-PEG IgM antibody secretion was examined 3 days after the preconditioning (Fig. 1B). When either PEGylated liposomes or the mixture of free Dox and PEGylated liposomes were administered, production of anti-PEG IgM antibody was increased about 6-fold compared with the baseline level obtained for the PBS group. Whereas, when the mice were injected with the PEG–Dox liposomes, the production did not increase at all.

3.2. Imaging of biodistribution of PEGylated liposomes with PPIS

To assess the ABC phenomenon non-invasively, we next examined the change in the real-time distribution of PEGylated liposomes by use of PPIS. [^{18}F]-Labeled PEGylated liposomes were intravenously administered to the mice that had been pretreated with PEGylated liposomes, PEG–Dox liposomes or PBS 3 days before, and the biodistribution was imaged (Fig. 2). The biodistribution of [^{18}F]-labeled PEGylated liposomes was imaged for 60 min, and the images were integrated into 1–30 and 31–60 min composite images. In the 1–30 min image, weak [^{18}F] signals were observed in the lung, spleen, kidney and bladder, and strong signals were detected in the liver, particularly in the mice pretreated with PEGylated liposomes. In the 31–60 min image, these signals were reduced in the lung, spleen, kidney and liver in the groups pretreated with PBS or PEG–Dox, and were significantly increased in the bladder in both groups. However, relatively strong signals remained in the group pretreated with the PEGylated liposomes.

3.3. Induction of ABC phenomenon in BALB/c nu/nu mice

BALB/c *nu/nu* (T cell-deficient) mice were preadministered PBS, PEGylated liposomes or PEG–Dox ones to clarify the role of T cells in the induction of the ABC phenomenon. In the mice pretreated with PEGylated liposomes, the amount of PEGylated liposomes significantly decreased in the plasma and significantly increased in the liver. This indicates that the ABC phenomenon was induced in BALB/c *nu/nu* mice (Fig. 3A). Consistent with the data for BALB/c mice, the pretreatment with PEG–Dox liposomes did not alter the pharmacokinetics of the test-dose PEGylated liposomes in these BALB/c *nu/nu* mice. The anti-PEG IgM antibody production was significantly increased in the mice pretreated with the PEGylated but not PEG–Dox liposomes (Fig. 3B). All results obtained for the BALB/c *nu/nu* mice were similar to those obtained for the BALB/c ones.

3.4. Significant role of B cells in the ABC phenomenon

Since T cells did not seem to be involved in the induction of the ABC phenomenon, we next determined the function of B cells in this phenomenon by using SCID mice, which are known to be deficient in both T and B cells. The biodistribution of test-dose PEGylated liposomes in BALB/c SCID mice was determined. As a result, any preadministrations (PEGylated liposomes, PEG–Dox liposomes, or PBS) did not alter the pharmacokinetics of the test-dose PEGylated liposomes. These results indicate that the ABC phenomenon was not induced in BALB/c SCID mice and that B cells play an important role in the induction of the ABC phenomenon (Fig. 4A). In addition, anti-PEG IgM antibody was not detected in any of the BALB/c SCID groups (Fig. 4B).